www.nature.com/aps

Acta Pharmacologica Sinica

ARTICLE

Platelet CFTR inhibition enhances arterial thrombosis via increasing intracellular Cl^- concentration and activation of SGK1 signaling pathway

Han-yan Yang[1], Chao Zhang[1], Liang Hu[2], Chang Liu[1], Ni Pan[1,3], Mei Li[4], Hui Han[1], Yi Zhou[5], Jie Li[6], Li-yan Zhao[7], Yao-sheng Liu[1], Bing-zheng Luo[5], Xiong-qing Huang[8], Xiao-fei Lv[1], Zi-cheng Li[1], Jun Li[1], Zhi-hong Li[1], Ruo-mei Wang[9], Li Wang[10], Yong-yuan Guan[1], Can-zhao Liu[11], Bin Zhang[5] and Guan-lei Wang[1]

Platelet hyperactivity is essential for thrombus formation in coronary artery diseases (CAD). Dysfunction of the cystic fibrosis transmembrane conductance regulator (CFTR) in patients with cystic fibrosis elevates intracellular Cl^- levels ($[Cl^-]_i$) and enhanced platelet hyperactivity. In this study, we explored whether alteration of $[Cl^-]_i$ has a pathological role in regulating platelet hyperactivity and arterial thrombosis formation. CFTR expression was significantly decreased, while $[Cl^-]_i$ was increased in platelets from CAD patients. In a $FeCl_3$-induced mouse mesenteric arteriole thrombosis model, platelet-specific Cftr-knockout and/or pre-administration of ion channel inhibitor CFTRinh-172 increased platelet $[Cl^-]_i$, which accelerated thrombus formation, enhanced platelet aggregation and ATP release, and increased $P2Y_{12}$ and PAR4 expression in platelets. Conversely, Cftr-overexpressing platelets resulted in subnormal $[Cl^-]_i$, thereby decreasing thrombosis formation. Our results showed that clamping $[Cl^-]_i$ at high levels or Cftr deficiency-induced $[Cl^-]_i$ increasement dramatically augmented phosphorylation (Ser422) of serum and glucocorticoid-regulated kinase (SGK1), subsequently upregulated $P2Y_{12}$ and PAR4 expression via NF-κB signaling. Constitutively active mutant $S422^D$ SGK1 markedly increased $P2Y_{12}$ and PAR4 expression. The specific SGK1 inhibitor GSK-650394 decreased platelet aggregation in wildtype and platelet-specific Cftr knockout mice, and platelet SGK1 phosphorylation was observed in line with increased $[Cl^-]_i$ and decreased CFTR expression in CAD patients. Co-transfection of $S422^D$ SGK1 and adenovirus-induced CFTR overexpression in MEG-01 cells restored platelet activation signaling cascade. Our results suggest that $[Cl^-]_i$ is a novel positive regulator of platelet activation and arterial thrombus formation via the activation of a $[Cl^-]_i$-sensitive SGK1 signaling pathway. Therefore, $[Cl^-]_i$ in platelets is a novel potential biomarker for platelet hyperactivity, and CFTR may be a potential therapeutic target for platelet activation in CAD.

Keywords: coronary artery disease; thrombosis; platelet; CFTR; intracellular chloride; SGK1

Acta Pharmacologica Sinica (2022) 43:2596–2608; https://doi.org/10.1038/s41401-022-00868-9

INTRODUCTION

Platelet activation and aggregation play critical roles in arterial thrombosis and are the primary pathogenic cause of arterial thrombotic diseases, including coronary artery diseases (CADs) [1, 2]. Hemostasis and pathological thrombus formation involve platelet surface receptors (e.g., glycoproteins and G-protein coupled receptors (GPCRs)). The pharmacological blockage of these surface receptors is an effective antiplatelet therapy for the treatment and prevention of arterial thrombosis. However, new therapeutic agents that target key steps in platelet activation to prevent arterial thrombosis remain warranted [3–5].

Abnormal chloride ion (Cl^-) transport plays a pivotal role in the pathogenesis of cardiovascular diseases [6, 7]. Low serum chloride is a biomarker and predictor of mortality in patients with heart failure and pulmonary arterial hypertension [8, 9]. Moreover, altered Cl^- transport is associated with platelet activation [10, 11]. However, whether alterations in $[Cl^-]_i$ occur in platelets as part of CAD pathogenesis, as well as the mechanism by which altered Cl^- transport leads to platelet activation and thrombus formation remain to be determined.

Cystic fibrosis transmembrane conductance regulator (CFTR), a cAMP-dependent chloride channel, participates in platelet

[1]Department of Pharmacology, Zhongshan School of Medicine, Sun Yat-sen University, Guangzhou 510080, China; [2]Academy of Integrative Medicine, Shanghai University of Traditional Chinese Medicine, Shanghai 201203, China; [3]Institute of Pediatrics, Guangzhou Women and Children's Medical Center affiliated to Guangzhou Medical College, Guangzhou 510623, China; [4]VIP Healthcare Center, the Third Affiliated Hospital of Sun Yat-sen University, Guangzhou 510630, China; [5]Guangdong Cardiovascular Institute, Guangdong Provincial People's Hospital, Guangdong Academy of Medical Sciences, Guangzhou 510080, China; [6]Department of Anesthesiology, The Second Affiliated Hospital of Guangzhou University of Chinese Medicine, Guangzhou 510120, China; [7]Department of Pharmacy, The First Affiliated Hospital of Sun Yat-sen University, Guangzhou 510080, China; [8]Department of Anesthesiology, the First Affiliated Hospital, Sun Yat-sen University, Guangzhou 510080, China; [9]School of Computer Science and Engineering, Sun Yat-sen University, Guangzhou 510006, China; [10]Division of Biological Sciences, University of California, San Diego, La Jolla, CA, USA and [11]Department of Cardiovascular Medicine, Translational Medicine Research Center, Zhujiang Hospital, Southern Medical University, Guangzhou 510280, China
Correspondence: Guan-lei Wang (wangglei@mail.sysu.edu.cn) or Bin Zhang (drbinzhang@gdph.org.cn) or Can-zhao Liu (liucanzhao0521@163.com)
These authors contributed equally: Han-yan Yang, Chao Zhang, Liang Hu

Received: 17 October 2021 Accepted: 17 January 2022
Published online: 3 March 2022

function [12]. The mutations in CFTR cause cystic fibrosis (CF), a recessively inherited and lethal disease. Platelets derived from CF patients demonstrate abnormal platelet $[Cl^-]_i$ concentration and platelet hyperactivity [13]. Recently, the role of CFTR in platelet hyperactivation has been identified in platelet-specific Cftr knockout mice, while CFTR deletion was shown to drive CF lung inflammatory responses and impair bacterial clearance [14]. However, the role of the CFTR chloride channel and CFTR-mediated Cl^- transport in thrombus formation remains unknown, while data on the pathophysiological significance of CFTR regarding platelet activation and thrombus formation in patients with CADs at a risk of thrombosis are limited.

In this study, we employ platelet-specific Cftr-knockout and overexpressing murine models to demonstrate that CFTR is responsible for increasing intracellular Cl^- levels ($[Cl^-]_i$) during platelet activation and thrombus formation. Moreover, we use site-specific mutation and adenovirus-mediated CFTR cDNA overexpression to determine how serum and glucocorticoid-regulated kinase (SGK1), an important regulator of platelet activation, is activated by $[Cl^-]_i$ which potentiates $P2Y_{12}$ and PAR4 expression via NF-κB signaling. Our mechanistic analysis suggests that SGK1 may function as a Cl^--sensitive signal transducer required for $[Cl^-]_i$-mediated platelet activation and thrombosis.

MATERIALS AND METHODS

Reagents

The sources of reagents are indicated in Table S1. Detailed methods and any associated references are provided in the online-only Supplemental Material.

Patient characterization

The study was conducted in accordance with the Declaration of Helsinki and approved by the Ethics Committee of the Sun Yat-sen University (2020-024) and the Ethics Committee of the Guangdong Provincial People's Hospital (KY-2020-062-01-02). All individuals were enrolled from Guangdong Provincial People's Hospital and divided into the CAD and normal coronary artery (NCA) groups according to the diagnostic criteria used after coronary angiography [15]. The inclusion criterion for the CAD group stated that CAD must be confirmed by coronary angiography (≥50% vascular stenosis). Patients with normal coronary angiographies were included in the NCA group. Informed consents were obtained from all participants. Participant details are listed in Table S2, and additional information has been included in the online-only Supplementary Material.

Intracellular Cl^- measurement

$[Cl^-]_i$ was measured using a previously described procedure, with slight modifications [16]. Briefly, washed platelets were incubated with 5 mM N-(ethoxycarbonylmethyl)−6-methoxyquinolinium bromide (MQAE, Invitrogen) for 30 min at 37 °C in the dark, and then washed with Krebs HEPES (128 mM NaCl, 5 mM KCl, 1 mM $MgSO_4{\cdot}7H_2O$, 15 mM glucose, 20 mM HEPES, 2 mM $CaCl_2$, 296–298 mM mOsm, pH 7.4) before measurement. Fluorometric data were obtained at 37 °C using a spectrofluorometer (SpectraMax M5) at excitation and emission wavelengths of 355 and 460 nm, respectively. The cells were permeabilized using tributyltin (10 μM) and nigericin (7 μM) in a high-K^+ solution. The calibration curve was obtained by fitting fluorescence intensity corresponding to known Cl^- concentrations, and the $[Cl^-]_i$ platelet level was calculated accordingly [17].

Generation of CFTR mice

We successfully designed and constructed Cftr conditional knockout mice using Cre/loxP recombination, which was generated by Cyagen (Suzhou, China). The Cftr conditional knockout mouse construct schematic is shown in Fig. S1a. Briefly, platelet-specific Cftr knockout ($Cftr^{PKO}$) mice were generated by crossing $Cftr^{fl/fl}$ mice with Platelet factor 4-Cre recombinase (Pf4-Cre) transgenic mice. Pf4-Cre mice were purchased from the Jackson Laboratory (Bar Harbor, USA). In experiments using $Cftr^{PKO}$ mice, mice containing $Cftr^{fl/fl}$ and Pf4-Cre were considered $Cftr^{PKO}$, and mice containing $Cftr^{fl/fl}$ or $Cftr^{fl/+}$ with Pf4-Cre negative were considered Ctrl. The $Cftr^{PKO}$ mice were genotyped using polymerase chain reaction (PCR) with the flox and Cre primers (Table S3). Genotyping results and platelet-specificity of the animal genotypes are shown in Fig. S1b–d, and platelet CFTR expression was substantially decreased in $Cftr^{PKO}$ mice compared with that in the Ctrl mice.

CFTR-ROSA26 conditional overexpression mice were also designed and successfully constructed by Cyagen (Suzhou, China). The CFTR platelet-specific overexpression ($Cftr^{POE}$) mouse construct schematic is shown in Fig. S2a. The $Cftr^{POE}$ mice were generated by crossing Rosa26 $Cftr^{fl/fl}$ mice with Pf4-Cre mice. The $Cftr^{POE}$ mice were genotyped using PCR with flox and Cre primers (Table S3). In experiments using $Cftr^{POE}$ mice, mice containing Rosa26 $Cftr^{fl/fl}$ and Pf4-Cre were considered $Cftr^{POE}$, and mice containing Rosa26 $Cftr^{fl/fl}$ or Rosa26 $Cftr^{fl/+}$ with Pf4-Cre negative were considered Ctrl. Genotyping results and platelet-specificity of the animal genotypes are shown in Fig. S2b–d, and platelet CFTR expression was substantially increased in $Cftr^{POE}$ mice compared to that in the Ctrl mice.

All $Cftr^{PKO}$, $Cftr^{POE}$, and their corresponding controls, as well as C57BL/6 J mice in the present study were 8-16 weeks old and sex, age, and body weight matched. C57BL/6 J mice were obtained from the Laboratory Animal Center of Sun Yat-sen University and intravenously injected with the selective CFTR inhibitor, CFTRinh-172 (2 mg/kg every day), 24 h before the experiments; mice injected with the same volume of saline containing DSMO served as the control. The dose of CFTRinh-172 was chosen based on previous reports, and the exacerbating effects of CFTRinh-172 on thrombosis was confirmed in our preliminary experiments [18].

All experimental procedures were approved by the Sun Yat-sen University Animal Care and Use Committee (No. SYSU-IACUC-2020-000446) and were in accordance with the "Guide for the Care and Use of Laboratory Animals" issued by the Ministry of Science and Technology of China, and conformed to the guidelines from Directive 2010/63/EU of the European Parliament on the protection of animals used for scientific purposes. The mice were anesthetized with an intraperitoneal injection of sodium pentobarbital (30 mg/kg) before performing any procedures. After the completion of all experiments, the mice were euthanized via cervical dislocation. All mice used were of the C57BL/6 J background and housed in the laboratory animal center of Sun Yat-sen University.

Statistical analysis

Data are presented as mean ± SEM. Statistical significance between the experimental groups was analyzed using unpaired *t*-tests. Three or more groups were compared using one-way analysis of variance, followed by Dunnett's multiple comparisons *post-hoc* test with 95% CI. Partial correlation analysis was used to examine the association between CFTR expression and platelet aggregation induced by ADP or thrombin. The statistical significance was evaluated using Prism software (GraphPad 8.0 Software, San Diego, CA, USA). Values with $P < 0.05$ were considered statistically significant. *ns* indicates non-significance ($P > 0.05$).

RESULTS

Elevated $[Cl^-]_i$ induced by CFTR deficiency participates in platelet aggregation in CAD

Abnormal transport of Cl^- is a risk factor for cardiovascular diseases. To determine the dynamics of Cl^- in the platelets of CAD

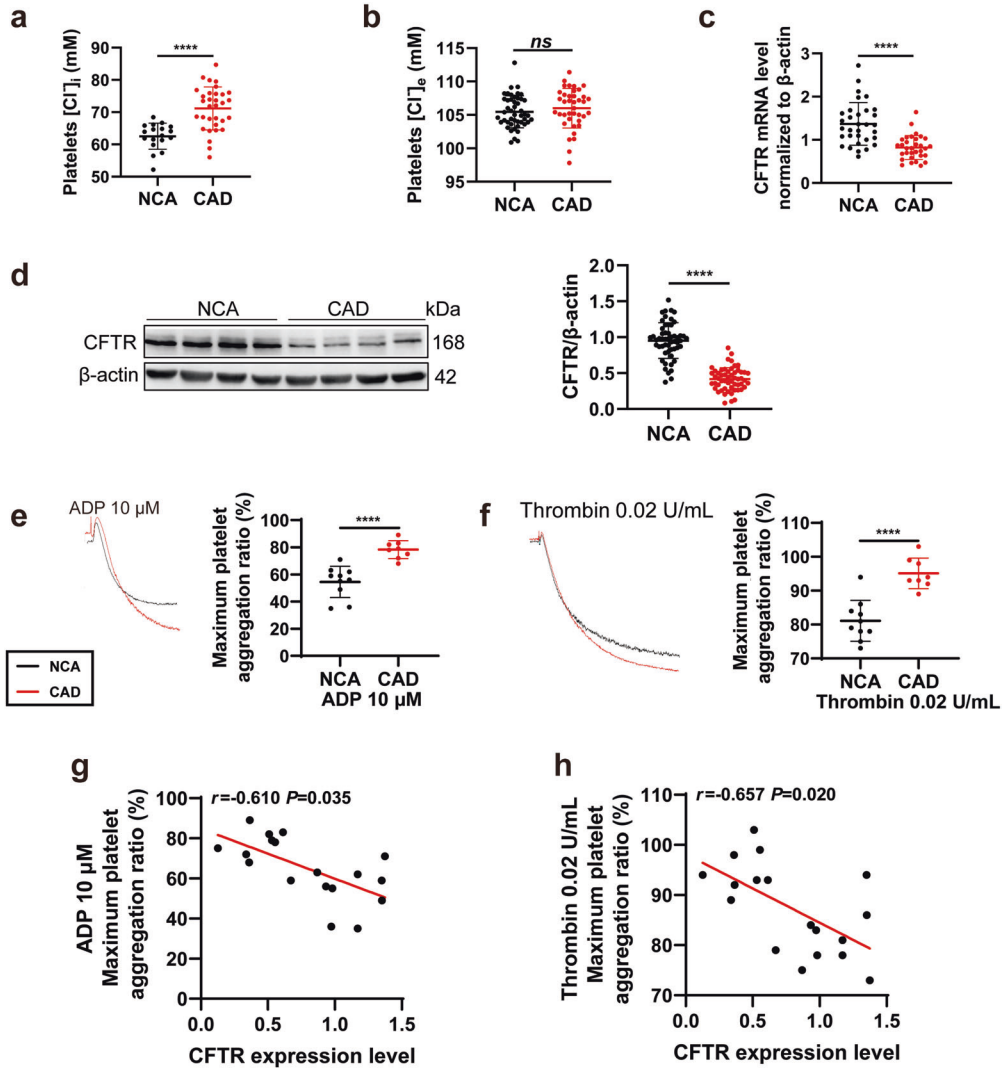

Fig. 1 CFTR-dependent $[Cl^-]_i$ is associated with platelet aggregation during CAD. The study subjects were grouped into normal coronary artery (NCA) and coronary artery disease (CAD) after coronary angiography. Washed platelets were collected from CAD patients and NCA controls. **a** $[Cl^-]_i$ was analyzed using the chloride indicator MQAE probe. (NCA, $n = 18$ *vs* CAD, $n = 32$; unpaired *t* test). **b** $[Cl^-]_e$ was analyzed using the ion-selective electrode method. (NCA, $n = 47$ *vs* CAD, $n = 39$; unpaired *t* test). **c** qRT-PCR analysis of *CFTR* mRNA expression. (NCA, $n = 32$ *vs* CAD, $n = 32$; unpaired *t* test). **d** Western blot analysis of CFTR protein expression. (NCA, $n = 54$ *vs* CAD, $n = 55$; unpaired *t* test). **e**, **f**, Aggregation of washed platelets in response to 10 μM ADP or 0.02 U/mL Thrombin. (NCA, $n = 10$ *vs* CAD, $n = 8$; unpaired *t* test). **g-h**, The correlation between the aggregation ratio and CFTR protein expression in platelets from NCA and CAD groups (In total, 18 samples from experiment **e**, **f**). *r* and *P* values by Partial correlation analysis are presented. Data are shown as mean ± SEM; $^{****}P < 0.0001$. ns not significant

patients, $[Cl^-]_i$ and extracellular Cl^- concentration ($[Cl^-]_e$) of platelets was measured. Intriguingly, platelet $[Cl^-]_i$ from CAD patients (71.9 ± 6.8 mM) was markedly increased compared to that from NCA subjects (62.5 ± 4.1 mM; Fig. 1a). However, no significant differences were observed in $[Cl^-]_e$ between the CAD and NCA groups (Fig. 1b).

Since Cl^- transport is regulated by chloride channels, we next determined the chloride channels responsible for increasing $[Cl^-]_i$ in CAD platelets. CFTR, LRRC8A, and TMEM16A are well recognized as principal molecular components of CFTR Cl^-, volume-regulated Cl^-, and Ca^{2+}-activated Cl^- channels, respectively [6, 19–22]. We found that the mRNA and protein levels of CFTR in platelets from CAD patients were significantly lower than those in NCA subjects (Fig. 1c, d); yet the expression levels of LRRC8A and TMEM16A were not altered at either the mRNA or protein levels in CAD patients (Fig. S3). In addition, the whole-cell patch clamp recording showed a CFTR-dependent Cl^- current in the human megakaryocytic cell line (MEG-01) during the resting state, which was effectively blocked by CFTRinh-172, a selective CFTR Cl^- channel inhibitor (Fig. S4a). Immunofluorescence imaging confirmed that CFTR was highly expressed in MEG-01 cells (Fig. S4b). These results suggested that Cl^- transport via the CFTR chloride channel is indeed required for Cl^- dynamics in platelets.

In line with the prothrombotic state in CAD, platelet aggregation in response to adenosine diphosphate (ADP) and thrombin was enhanced in patients with CAD compared with NCA subjects (Fig. 1e, f). The partial correlation analysis is used to assess the association between two variables without specifying the direction of such association, while holding other variables constant [23, 24]. We performed partial correlation analysis to examine the association between CFTR expression and platelet aggregation induced by ADP or thrombin. CFTR expression in human platelets was negatively correlated with platelet aggregation induced by ADP or thrombin, when the six confounders (total cholesterol, LDL, HDL, blood platelet count, β-blockers, statins) remained constant (Fig. 1g, h, Table S2). These findings suggest that the abnormal

$[Cl^-]_i$ in platelets from CAD patients may be due to dysfunctional CFTR chloride channels or decreased CFTR expression, implying that CFTR plays an important role in platelet functioning during CAD.

Megakaryocyte/platelet-specific Cftr-deficient mice, and CFTRinh-172 exacerbates arterial thrombus formation in vivo

We next investigated the role of CFTR in arterial thrombus formation in vivo using a $FeCl_3$-induced mouse mesenteric arteriole thrombosis model. Thrombus formation was monitored in real-time using fluorescence microscopy. To characterize the specific role of CFTR in platelet function, we engineered Cftr ($Cftr^{fl/fl}$) floxed alleles and crossed $Cftr^{fl/fl}$ mice with Pf4-Cre mice, which expressed Cre-recombinase exclusively in the megakaryocytic lineage, to generate platelet-specific Cftr knockout mice ($Cftr^{PKO}$, Fig. S1). Compared with the control (Ctrl: $Cftr^{fl/fl}$; $Cftr^{fl/+}$) mice, $Cftr^{PKO}$ mice showed increased thrombus formation in the $FeCl_3$-induced mesenteric arteriole thrombosis model (Fig. 2a). The time to the first thrombus formation in the mesenteric arteriole was significantly shorter in $Cftr^{PKO}$ mice than in Ctrl mice ($Cftr^{PKO}$, 6.5 ± 1.2 min *vs.* Ctrl, 9.1 ± 3.1 min, $P < 0.05$; Fig. 2b). Additionally, the maximum thrombus size in $Cftr^{PKO}$ mice was larger than that in Ctrl mice [$Cftr^{PKO}$, (173.0 ± 35.0) × 10^3 μm^2 vs Ctrl, (91.2 ± 27.2) × 10^3 μm^2; $P < 0.001$; Fig. 2b]. As a CFTR chloride channel blocker, CFTRinh-172 inhibits CFTR chloride channel-mediated Cl^- transport by binding to the nucleotide binding domains of the CFTR protein rather than affecting CFTR expression (Fig. S5) [18, 25]. Consistent with the results from CFTR genetic ablation in mice, pharmacological inhibition of CFTR by CFTRinh-172 intravenous injection in wild-type mice also accelerated $FeCl_3$-induced thrombus formation in mesenteric arteries, reflected by a shorter time to the first thrombus formation and an increased maximum thrombus size (Fig. 2c, d). Together, these findings indicate that platelet CFTR is important for arterial thrombus formation in vivo.

To investigate the role of CFTR in hemostasis, we examined tail blood loss and bleeding time in $Cftr^{PKO}$ and Ctrl littermates. The volume of tail blood loss was significantly decreased in $Cftr^{PKO}$ mice compared with that in Ctrl mice ($Cftr^{PKO}$ 108.5 ± 64.1 μL vs. Ctrl 408.3 μL ± 309.2 μL, Fig. 2e), however, bleeding times were indistinguishable between Ctrl and $Cftr^{PKO}$ mice (Fig. 2f). These findings suggest that CFTR plays a minor role in hemostasis.

We further measured hematologic parameters, including platelet counts, mean platelet volume, hemoglobin concentration, and coagulation parameters, and obtained similar values in Ctrl and $Cftr^{PKO}$ mice (Tables S4 and S5, $P > 0.05$). $Cftr^{PKO}$ mice exhibited increased platelet surface CD62P compared with Ctrl mice (Fig. 2g), suggesting that CFTR regulates platelet activation.

Electron microscopy did not reveal any ultrastructural abnormalities, including morphological changes in the open canalicular system or the number of α-granules and dense granules in platelets of $Cftr^{PKO}$ mice (Fig. 2h).

Megakaryocyte/platelet-specific Cftr-deficient mice, and CFTRinh-172 enhances platelet aggregation and dense granule ATP release induced by agonists

We further investigated whether CFTR regulates platelet aggregation and ATP release in vitro. As shown in Fig. 3, maximum platelet aggregation in response to ADP (2.5, 5, and 10 μM; Fig. 3a), thrombin at lower dosages (0.01 and 0.02 U/mL; Fig. 3b), and collagen (0.5 μg/mL; Fig. 3d) was significantly enhanced in $Cftr^{PKO}$ platelets compared with that in the controls. Under these conditions, ATP release induced by thrombin (0.01 and 0.02 U/mL) and collagen (0.5 μg/mL) was also significantly enhanced in $Cftr^{PKO}$ platelets (Fig. 3c, e). However, there were no differences in neither the maximum platelet aggregation (Fig. 3b), nor in the ATP release (Fig. 3c) in response to a relatively high dose of thrombin (0.05 U/mL) between $Cftr^{PKO}$ and the corresponding controls. In addition, CFTRinh-172 produced similar effects on platelet aggregation and ATP release in wild-type mice, as observed in $Cftr^{PKO}$ platelets (Fig. 3f–h). These data indicate that CFTR deficiency enhanced ATP release and platelet aggregation induced by agonists.

Platelet-specific Cftr overexpression ameliorates platelet aggregation, ATP release, and thrombosis

To determine the effects of CFTR on platelets during platelet activation and arterial thrombosis, we constructed a conditional knock-in mouse line that contained a CAG promoter followed by a "loxp-Stop-loxp-Kozak-Cftr coding region" cassette using a CRISPR/Cas9 genome-targeting system and crossed these mice with Pf4-Cre mice to generate platelet-specific Cftr-overexpressing mice ($Cftr^{POE}$; Fig. S2). Overexpression of CFTR in platelets significantly alleviated thrombus formation and vessel occlusion induced by $FeCl_3$ injury (Fig. 4a). The time to the first thrombus formation in the mesenteric arteriole was significantly delayed ($Cftr^{POE}$, 12.3 ± 2.7 min vs. Ctrl, 8.8 ± 1.8 min, $P < 0.01$; Fig. 4b), and the maximum thrombus size was also reduced in $Cftr^{POE}$ mice [$Cftr^{POE}$, (34.81 ± 9.41) × 10^3 μm^2 vs. Ctrl, (100.04 ± 24.11) × 10^3 μm^2; $P < 0.0001$; Fig. 4b]. However, there was no significant difference in the bleeding time or tail blood loss between $Cftr^{POE}$ and Ctrl mice (Fig. S6).

In contrast to $Cftr^{PKO}$ mice, the maximum platelet aggregation in response to ADP (2.5, 5, and 10 μM; Fig. 4c), thrombin at lower dosages (0.01 and 0.02 U/mL; Fig. 4d), and collagen (0.5 μg/mL; Fig. 4f) was significantly reduced in $Cftr^{POE}$ platelets. Under these conditions, ATP release induced by thrombin (0.01 and 0.02 U/mL) and collagen (0.5 μg/mL) was also significantly reduced in $Cftr^{POE}$ platelets (Fig. 4e, g). There were no differences in maximum platelet aggregation in response to a relatively high dose of thrombin (0.05 U/mL) in $Cftr^{POE}$ mice and their corresponding controls (Fig. 4d). However, ATP release induced by thrombin (0.05 U/mL) was reduced in $Cftr^{POE}$ platelets compared with that in the controls (Fig. 4e). These data suggest that CFTR overexpression ameliorates platelet aggregation, ATP release, and thrombosis.

CFTR regulates platelet aggregation through the $P2Y_{12}$ and PAR4 signaling pathway

Platelet surface receptors, $P2Y_1$/$P2Y_{12}$, PAR4, and TP, and membrane glycoproteins, CD41 (GPIIb/IIIa), CD61 (GPIIIa), CD42b (GPIbα), and GPVI, are critical for platelet function [2, 4, 26]. Therefore, we screened platelet surface proteins in $Cftr^{PKO}$ and $Cftr^{POE}$ platelets and found no significant differences in the surface expression of the platelet glycoproteins (CD41, CD61, CD42b, and GPVI; Fig. 5a, b). Meanwhile, the GPCR of $P2Y_{12}$ and PAR4 were significantly upregulated in $Cftr^{PKO}$ mice compared with that in Ctrl mice (Fig. 5c, d). In line with the results of genetically modified mice, protein expressions of $P2Y_{12}$ and PAR4 were also significantly augmented in CAD platelets (Fig. S7). However, there was no significant difference in the mRNA expression of *$P2Y_1$* and *TP* in platelets from $Cftr^{PKO}$ and Ctrl mice (Fig. 5e). Conversely, $Cftr^{POE}$ downregulated $P2Y_{12}$ and PAR4 expression (Fig. 5f, g). Similar to those in $Cftr^{PKO}$ mice, the protein level of GPVI and the mRNA levels *$P2Y_1$* and *TP* showed no changes in $Cftr^{POE}$ platelets compared with those in the Ctrl mice (Fig. 5h, i).

Therefore, we explored platelet activation and aggregation signaling pathways associated with $P2Y_{12}$ and PAR4. $P2Y_{12}$ and PAR4 activation induces platelet activation and aggregation through the PI3K/Akt pathway. The phosphorylation of PI3K and Akt was enhanced in $Cftr^{PKO}$ platelets but reduced in $Cftr^{POE}$ platelets (Fig. 5j–k and l, m). The results of the CFTR genetic ablation on $P2Y_{12}$ and PAR4-mediated platelet aggregation signaling pathway were consistent with those of $FeCl_3$-induced mesenteric arteriole thrombosis in $Cftr^{PKO}$ mice, suggesting that CFTR regulates platelet aggregation and thrombus formation via the $P2Y_{12}$ and PAR4 pathways.

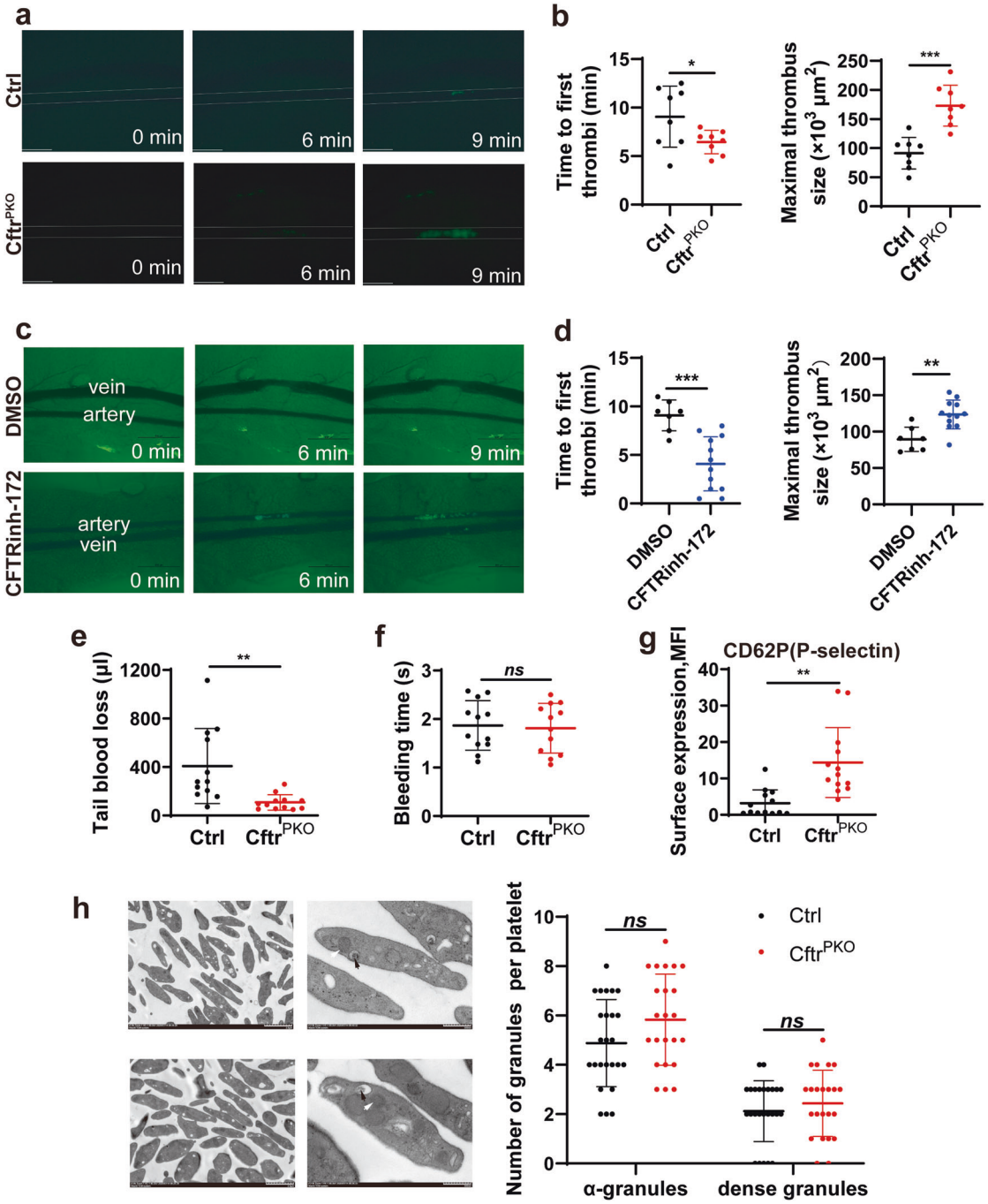

Fig. 2 CFTR regulates $FeCl_3$-induced mesenteric arteriole thrombosis. a Representative images and time courses of $FeCl_3$-induced mesenteric arteriole thrombus formation in $Cftr^{PKO}$ and Ctrl mice. Time after $FeCl_3$-induced injury is indicated at the low right corner of each image. Scale bars, 500 μm. **b** Summary of the time to first thrombi and maximal thrombus size of arterioles from the result of $FeCl_3$-induced thrombosis in $Cftr^{PKO}$ and Ctrl mice in Fig. 2a. ($n = 8$ mice per group; unpaired t test). **c** WT mice were intravenously injected with CFTRinh-172 (2 mg/kg every day, 24 h) or the same volume of normal saline containing DSMO as a control before $FeCl_3$ injury. Representative images of $FeCl_3$-induced mesenteric arteriole thrombosis in WT mice treated with CFTRinh-172 or DMSO as recorded by real-time microscopy. Time after $FeCl_3$-induced injury is indicated at the low right corner of each image. Scale bars, 500 μm. **d** Summary of the time to first thrombi and maximal thrombus size of arterioles from the result of $FeCl_3$-induced thrombosis in WT mice treated with CFTRinh-172 or DMSO in Fig. 2c ($n =$ 7 or 12 mice per group; unpaired t test). **e**, **f** Tail blood loss and tail bleeding time parameters were investigated in $Cftr^{PKO}$ and Ctrl mice ($n = 12$ mice per group; unpaired t test). **g** Surface expression of CD62P (P-selectin) as determined using flow cytometry with PE-conjugated anti-mouse/rat CD62P in $Cftr^{PKO}$ and Ctrl mice ($n = 13$ mice per group; unpaired t test). **h** Representative electron microscopy images of platelet ultrastructure from Ctrl and $Cftr^{PKO}$ mice. Scale bars, 2.0 μm (top) and 500 nm (bottom). Quantification of α-granules (white arrow) and dense granules (black arrow) per platelet from Ctrl and $Cftr^{PKO}$ platelets. ($n = 23$–25; unpaired t test). Data are presented as mean ± SEM; $^*P < 0.05$, $^{**}P < 0.01$, and $^{***}P < 0.001$. ns not significant

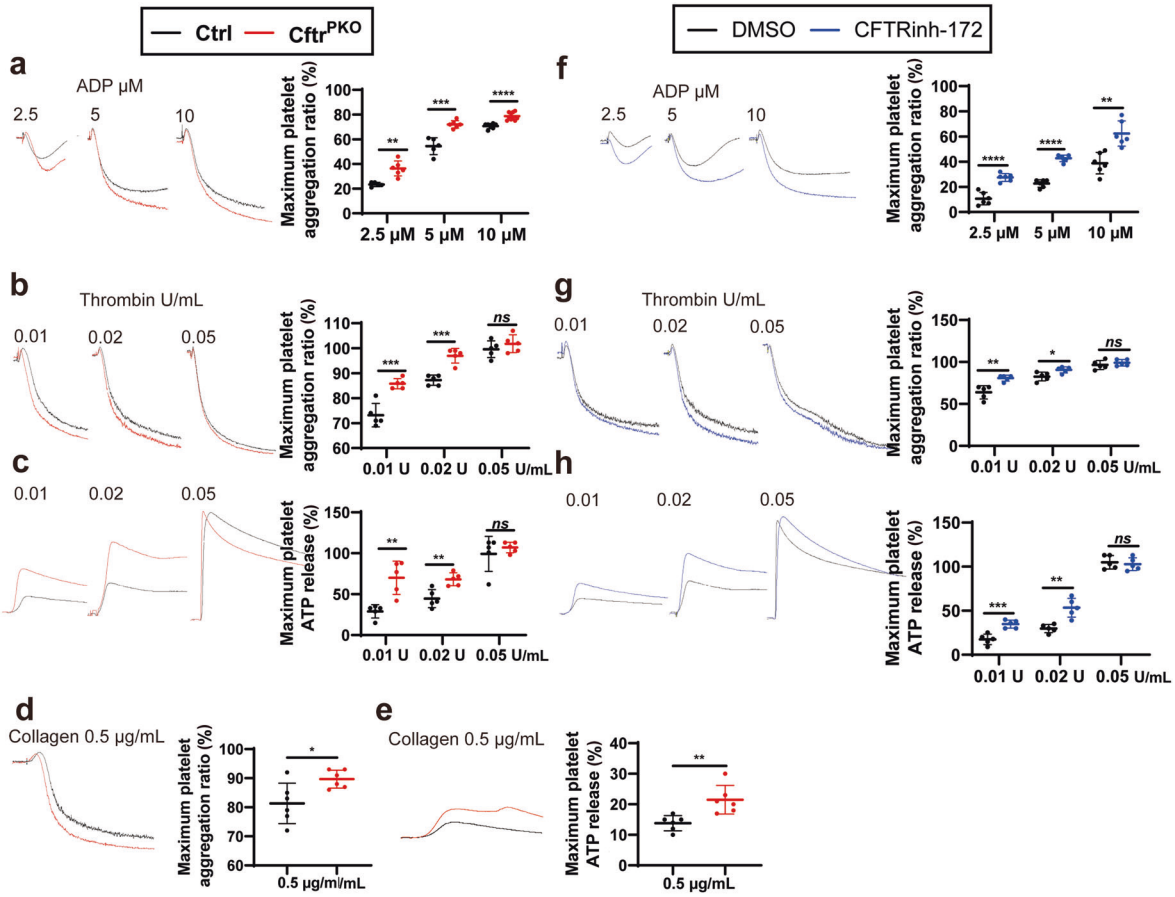

Fig. 3 $Cftr^{PKO}$ and CFTRinh-172 platelets display enhanced aggregation and ATP release. a–e Aggregation or ATP release of washed $Cftr^{PKO}$ and Ctrl platelets were stimulated with different concentrations of ADP (2.5, 5, or 10 μM) (**a**), thrombin (0.01, 0.02, or 0.05 U/mL) (**b**, **c**) and collagen (0.5 μg/mL) (**d**, **e**) at 37 °C under constant stirring. Representative tracings (left) and quantification graphs (right) are presented. (n = 5–10 mice per group; unpaired t test). **f–h**, WT mice were intravenously administered CFTRinh-172 (2 mg/kg every day, 24 h) or the same volume of normal saline containing DSMO as a control before stimulation. Washed platelets were stimulated with different concentrations of ADP (2.5, 5, or 10 μM) (**f**) and thrombin (0.01, 0.02, or 0.05 U/mL) (**g**, **h**) at 37 °C under constant stirring. Platelet aggregation and ATP release were monitored using an aggregometer. Representative tracings (left) and quantification graphs (right) were presented. (n = 5–6 mice per group; unpaired t test). Data are shown as mean ± SEM; *P < 0.05, **P < 0.01, ***P < 0.001, and ****P < 0.0001. ns not significant

Elevated $[Cl^-]_i$ induced by CFTR deficiency promotes platelet aggregation via SGK1 activation

We next investigated the molecular pathways underlying platelet activation in Cftr knockout and overexpressing mice. Based on the abnormally high $[Cl^-]_i$ in CAD platelets, we hypothesized that CFTR regulates platelet $[Cl^-]_i$. Hence, measurements of platelet $[Cl^-]_i$ from $Cftr^{PKO}$ and $Cftr^{POE}$ mice were performed using MQAE, a fluorescent indicator for intracellular Cl^-. The platelet $[Cl^-]_i$ of $Cftr^{PKO}$ mice was higher than that of Ctrl mice (Fig. 6a). In contrast, platelet $[Cl^-]_i$ in $Cftr^{POE}$ mice was much lower than that in Ctrl mice (Fig. 6b). As shown in Fig. 6c, incubation of circulating platelets from wild-type mice with CFTRinh-172 (5 μM) produced a time-dependent increase in $[Cl^-]_i$ with $[Cl^-]_i$ beginning to increase immediately after CFTRinh-172 administration, reaching its maximum level after 20 min (from 50.2 ± 1.8 mM to 73.6 ± 3.1 mM vs. from 49.6 ± 3.1 mM to 47.6 ± 2.2 mM, P < 0.0001, n = 10). These data indicate that *CFTR* genetic intervention or pharmacological inhibition of CFTR chloride channels could regulate platelet $[Cl^-]_i$.

Increasing evidence suggests that $[Cl^-]_i$ plays a role in modulating protein function and gene expression via activation of Cl^--sensitive kinases [16, 27, 28]. SGK1 plays an important role in platelet activation and thrombosis and is a potential Cl^--sensitive kinase in regulating multiple cellular functions [16, 29]. These findings suggest that CFTR-mediated Cl^- transport regulates platelet function via SGK1 activity. To determine whether $[Cl^-]_i$ could modulate SGK1 activity, we established an in vitro model with $[Cl^-]_i$ gradients in platelets by changing extracellular Cl^- concentrations [16]. SGK1 phosphorylation at Ser422 was upregulated by increasing platelet $[Cl^-]_i$ in a concentration-dependent manner (Fig. 6d). Moreover, SGK1 phosphorylation greatly increased in $Cftr^{PKO}$ platelets, but, decreased in $Cftr^{POE}$ circulating platelets (Fig. 6e, f). In line with the significant increase of platelet $[Cl^-]_i$ from CAD patients, increased SGK1 phosphorylation at Ser422 was observed in CAD platelets (Fig. 6g). In addition, GSK-650394, a specific SGK1 inhibitor, potently inhibited platelet aggregation and reversed the increased aggregation rates in $Cftr^{PKO}$ platelets (Fig. 6h). These results suggest that CFTR deficiency promoted platelet activation via elevated $[Cl^-]_i$ activating SGK1 signaling.

SGK1 transduces the $[Cl^-]_i$ signal from decreased CFTR to downstream NF-κB/$P2Y_{12}$ and PAR4 activation

Increased SGK1 activity (phosphorylation of SGK1 S422) in $Cftr^{PKO}$ platelets led us to address the role of $[Cl^-]_i$-sensitive, SGK1-dependent signaling in platelet activation and aggregation. The activation of SGK1 has been shown to phosphorylate IκBα and trigger its degradation, which in turn promotes nuclear translocation and activation of NF-κB, leading to the upregulation of Orai1-dependent store-operated Ca^{2+} entry [30, 31]. Given that NF-κB is the signaling molecule upstream of $P2Y_{12}$ and PAR4, we

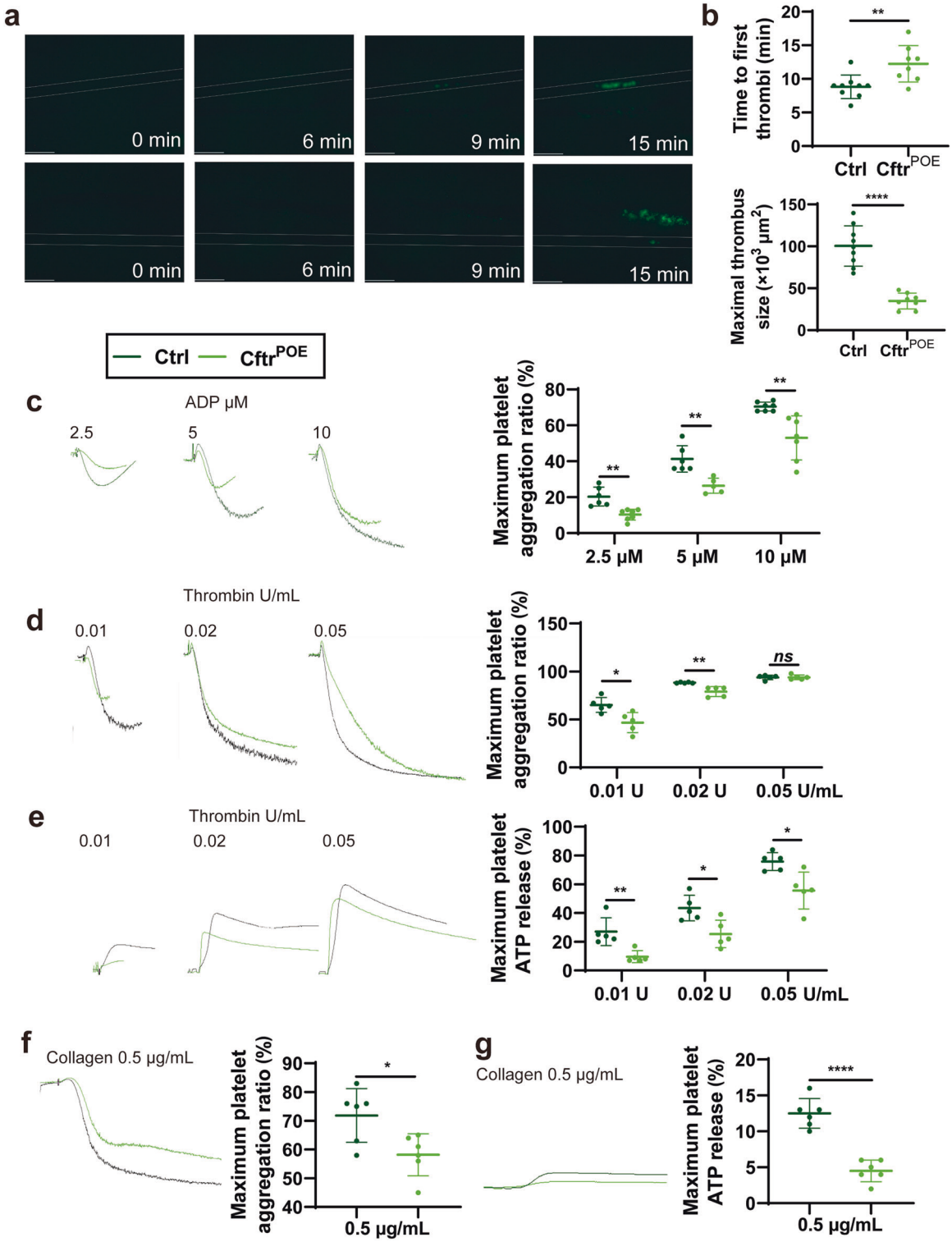

Fig. 4 Cftr^{POE} reduces thrombosis in vivo and decreases aggregation and ATP release in vitro. a Representative images and time courses of $FeCl_3$-induced mesenteric arteriole thrombus formation in Cftr^{POE} and Ctrl mice. Time after $FeCl_3$-induced injury is indicated at the low right corner of each image. Scale bars, 500 μm. **b** Summary of the time to first thrombi and maximal thrombus size of arterioles from the result of $FeCl_3$-induced thrombosis in Cftr^{POE} and Ctrl mice in Fig. 4a. ($n = 8$ or 9 mice per group; unpaired t test). **c**–**g** Aggregation or ATP release of washed Cftr^{POE} and Ctrl platelets were stimulated with different concentrations of ADP (2.5, 5, or 10 μM) (**c**), thrombin (0.01, 0.02, or 0.05 U/mL) (**d**, **e**) and collagen (0.5 μg/mL) (**f**, **g**) at 37 °C under constant stirring. Representative tracings (left) and quantification graphs (right) are presented ($n = 5$–7 mice per group; unpaired t test). Data are presented as mean ± SEM; $^*P < 0.05$, $^{**}P < 0.01$, and $^{****}P < 0.0001$. ns not significant

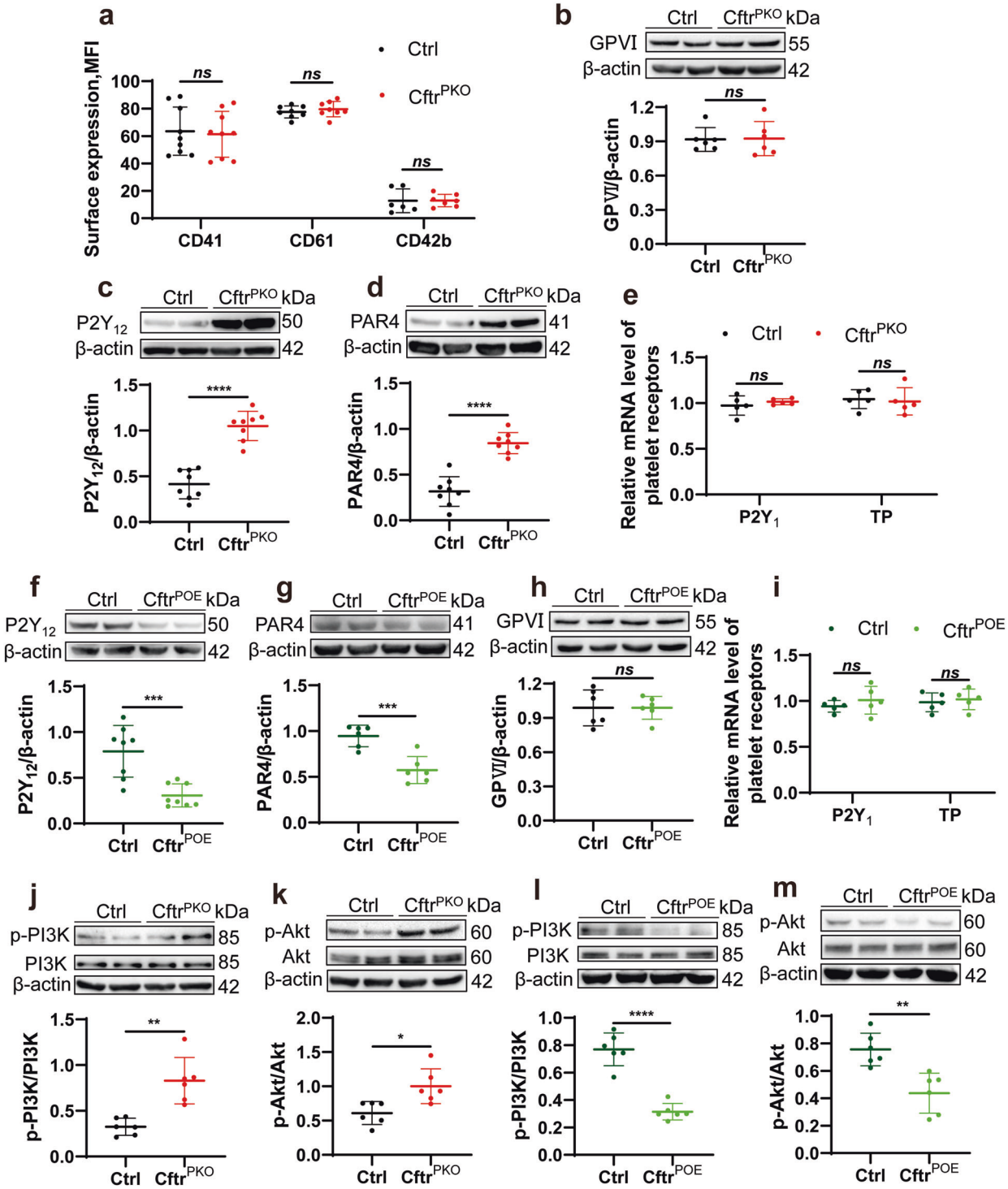

Fig. 5 CFTR regulates platelet aggregation through the $P2Y_{12}$ and PAR4 signaling pathway. a Surface expression of CD41, CD61, and CD42b in $Cftr^{PKO}$ and Ctrl platelets were detected using flow cytometry, and the values were expressed as mean fluorescence intensity (MFI) ($n = 6$–9 mice per group; unpaired *t* test). **b** Western blot analysis of GPVI expression in $Cftr^{PKO}$ and Ctrl platelets ($n = 6$ mice per group; unpaired *t* test). **c** Western blot analysis of $P2Y_{12}$ expression in $Cftr^{PKO}$ and Ctrl platelets ($n = 8$ mice per group; unpaired *t* test). **d** Western blot analysis of PAR4 expression in $Cftr^{PKO}$ and Ctrl platelets ($n = 8$ mice per group; unpaired *t* test). **e** qRT-PCR analysis of *$P2Y_1$* and *TP* mRNA expression in $Cftr^{PKO}$ and Ctrl platelets ($n = 5$ mice per group; unpaired *t* test). **f**, Western blot analysis of $P2Y_{12}$ expression in $Cftr^{POE}$ and Ctrl platelets ($n = 8$ mice per group; unpaired *t* test). **g** Western blot analysis of PAR4 expression in $Cftr^{POE}$ and Ctrl platelets ($n = 6$ mice per group; unpaired *t* test). **h** Western blot analysis of GPVI expression in $Cftr^{POE}$ and Ctrl platelets ($n = 6$ mice per group; unpaired *t* test). **i** qRT-PCR analysis of *$P2Y_1$* and *TP* mRNA expression in $Cftr^{POE}$ and Ctrl platelets ($n = 5$ mice per group; unpaired *t* test). **j**–**m**, Western blot analysis of total and phosphorylated PI3K and Akt protein expression in $Cftr^{PKO}$ (**j**–**k**), $Cftr^{POE}$ (**l**, **m**), and their age-matched Ctrl platelets ($n = 6$ mice per group; unpaired *t* test). Data are presented as mean ± SEM; $^*P < 0.05$, $^{**}P < 0.01$, $^{***}P < 0.001$, and $^{****}P < 0.0001$. ns not significant.

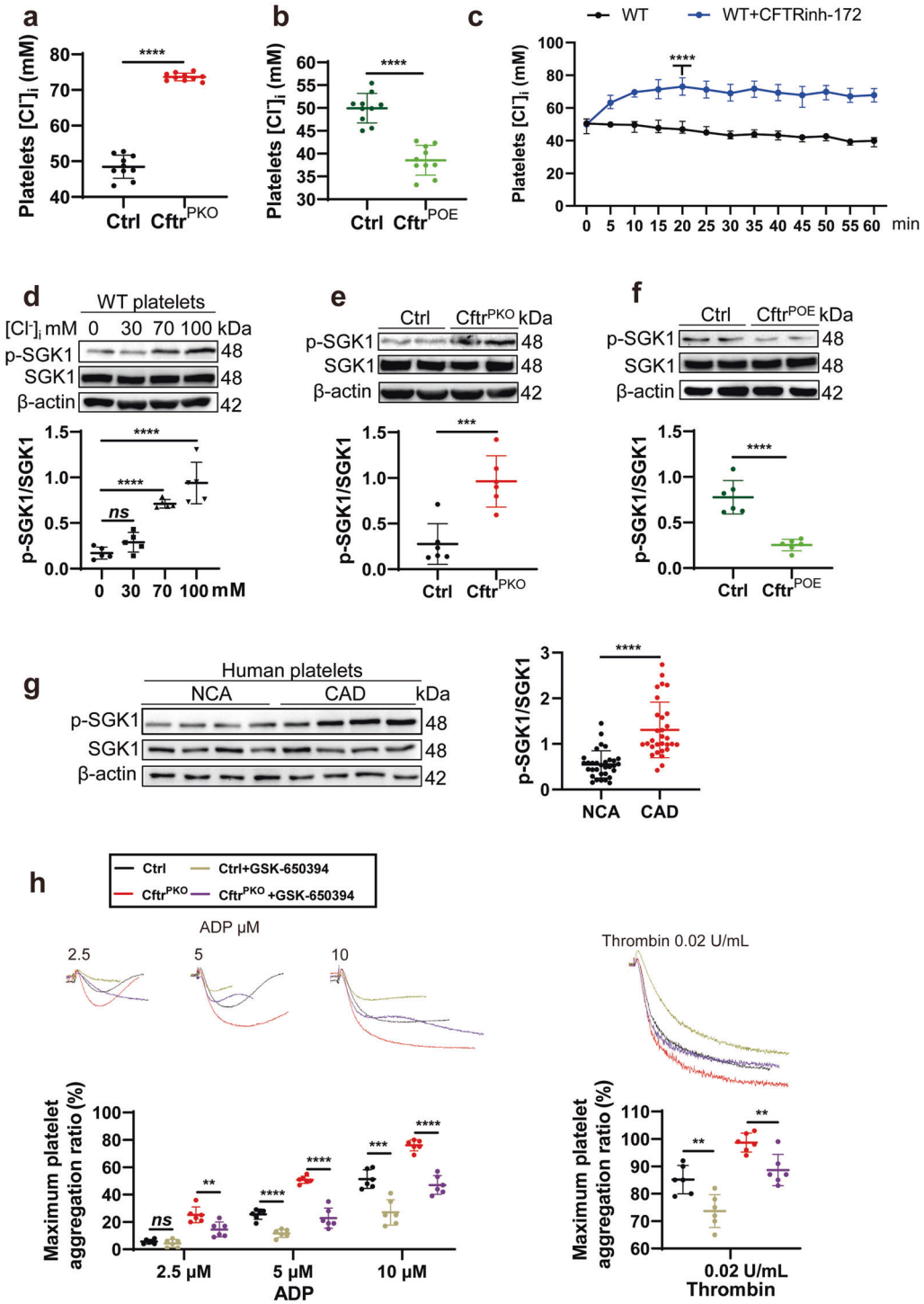

Fig. 6 CFTR-mediated $[Cl^-]_i$ regulates platelet aggregation via SGK1 activation. a, **b** $[Cl^-]_i$ in platelets from $Cftr^{PKO}$ (**a**), $Cftr^{POE}$ (**b**), and corresponding age-matched Ctrl mice ($n = 10$ mice per group; unpaired *t* test). **c**, Real-time change of platelets $[Cl^-]_i$ was measured in WT mice incubated with or without 5 μM CFTRinh-172 ($n = 10$ per group; unpaired *t* test). **d** Western blot analysis of total and phosphorylated SGK1 (S422) expressions in WT platelets stimulated with varying $[Cl^-]_i$ levels ($n = 5$ independent experiments; one-way ANOVA). **e**, **f** Western blot analysis of total and phosphorylated SGK1 (S422) expressions in $Cftr^{PKO}$ (**e**), $Cftr^{POE}$ (**f**), and their corresponding Ctrl platelets ($n = 6$ mice per group; unpaired *t* test). **g**, Western blot analysis of total and phosphorylated SGK1 (S422) expressions in platelets from patients with CAD and NCA subjects. (NCA, $n = 32$ vs. CAD, $n = 30$; unpaired *t* test). **h** Aggregation of $Cftr^{PKO}$ or Ctrl platelets stimulated with various concentrations of ADP (2.5, 5, and 10 μM) or thrombin (0.02 U/mL) following in vitro pre-incubation with/without GSK-650394 (1 μM) for 30 min. Representative tracings and quantification graphs are shown ($n = 6$ mice per group; unpaired *t* test). Data are mean ± SEM; $^{**}P < 0.01$, $^{***}P < 0.001$, and $^{****}P < 0.0001$. ns not significant.

hypothesized that CFTR-mediated $[Cl^-]_i$ influences $P2Y_{12}$ and PAR4 expression via the activation of SGK1-dependent IκBα/NF-κB. To test this, MEG-01 cells were transfected with a constitutively active mutant $S422^D$ SGK1 or an inactive mutant $S422^A$ SGK1 (Fig. S8a). $S422^D$ increased the expression of $P2Y_{12}$ and PAR4, which was reversed by $S422^A$ transfection (Fig. 7a). In addition, IκBα phosphorylation was increased in MEG-01 cells transfected with $S224^D$, but inhibited by $S422^A$ (Fig. 7b). Notably, neither $S422^D$ nor $S422^A$ affected CFTR expression or $[Cl^-]_i$ in MEG-01 cells (Fig. 7c–d), whereas CFTR genetic intervention affected SGK1 activity (Fig. 6e, f). Taken together, the results shown in Fig. 7a–d indicate that SGK1 acted downstream of CFTR-mediated signaling pathways in platelet activation, with no feedback regulation of platelet CFTR expression and $[Cl^-]_i$ after SGK1 activation.

To further verify the role of SGK1 and CFTR in platelet activation, CFTR overexpression adenovirus and the active SGK1 mutant $S422^D$ were co-transfected into MEG-01 cells (Fig. 7e, f, Fig. S8b). CFTR overexpression alone abolished IκBα activation and the subsequent expression of $P2Y_{12}$ and PAR4 (Fig. 7e, f) by decreasing SGK1 phosphorylation (Fig. S8b). The co-transfection of CFTR overexpressing adenovirus and S422D restored the platelet activation signaling cascade, which, had no effect on constitutively active SGK1 (Fig. 7e, f). These data support the notion that SGK1 is a downstream kinase of CFTR in $P2Y_{12}$ and PAR4-mediated platelet activation signaling pathways. Collectively, these data suggest that CFTR-mediated elevation of $[Cl^-]_i$ activates the phosphorylation of SGK1 and thereby potentiates the downstream IκBα/NF-κB/$P2Y_{12}$ and PAR4 platelet activation signaling pathway.

DISCUSSION

To the best of our knowledge, this is the first study to report that $[Cl^-]_i$ is increased, while CFTR protein expression is decreased, in platelets of patients with CAD with enhanced platelet aggregation, suggesting $[Cl^-]_i$ as a potential biomarker of thrombosis risk, and CFTR as a novel antiplatelet target for thrombotic diseases. By engineering constructed Cftr-knockout and -overexpressing mice, this study provides the first evidence of *CFTR* and CFTR chloride channels regulating platelet aggregation and platelet-mediated arterial thrombosis formation. The ablation of CFTR in platelets upregulated $[Cl^-]_i$ and accelerated $FeCl_3$-induced thrombus formation, whereas thrombus formation and vessel occlusion were ameliorated in Cftr-overexpressing mice, accompanied by downregulated platelet $[Cl^-]_i$. These results illustrate that CFTR-mediated platelet $[Cl^-]_i$ homeostasis is critical for platelet functioning.

Our results also showed that decreased CFTR expression increased platelet $[Cl^-]_i$, thereby enhancing $P2Y_{12}$ and PAR4 expression via an SGK1-dependent NF-κB pathway. Although previous studies have suggested that Cl^- transport is responsible for platelet activation [10, 32], whether alteration in $[Cl^-]_i$ occurs in platelets during CAD pathogenesis remains to be determined. Here, platelets from CAD patients showed markedly elevated $[Cl^-]_i$, accompanied by elevated platelet aggregation, as well as $P2Y_{12}$ and PAR4 expression. Furthermore, the results obtained from $Cftr^{PKO}$ directly show that the basal platelet $[Cl^-]_i$ upregulated by CFTR deficiency is essential for platelet activation and aggregation as well as arterial thrombus formation. Additionally, increased $[Cl^-]_i$ was observed in platelets from $Cftr^{PKO}$ and wildtype mice treated with CFTRinh-172, which activated the downstream SGK1/NF-κB signaling to potentiate $P2Y_{12}$ and PAR4 expression. Moreover, increased SGK1 activation induced by elevated $[Cl^-]_i$ was abolished in Cftr-overexpressing mice. These data indicate that CFTR is an important chloride channel responsible for platelet Cl^- homeostasis, which is essential for maintaining platelet functions. Moreover, $[Cl^-]_i$ may effectively predict risk of cardiovascular events; that is, maintenance of platelet Cl^- homeostasis, mediated by CFTR, significantly reduces the risk of experiencing a cardiovascular event. Although platelets from patients with CAD expressed similar levels of the well-recognized chloride channel proteins, LRRC8A and TMEM16A, as NCA subjects, we cannot exclude the possibility that other unknown Cl^- transporters might have contributed to the platelet activation and thrombus formation under CAD conditions.

$[Cl^-]_i$, similar to other ion concentrations, serves as an intracellular signal [16, 27, 28]. Our study showed that SGK1 kinase activity is increased in a Cl^- -dependent manner. SGK1 is a kinase with Cl^--sensing properties; SGK1 phosphorylation at Ser422 increases platelet activation and granule biogenesis [33]. Previous studies on the role of SGK1 in platelet functioning have focused largely on the SGK1-sensitive regulation of Orai1-dependent store-operated $[Ca^{2+}]_i$-sensitive Ca^{2+} entry signaling pathways. Thus, it is unclear how SGK1 is activated in platelet activation. Here, our results provide the first evidence that SGK1 is activated by higher $[Cl^-]_i$ induced by CFTR deficiency in platelets, which then potentiates $P2Y_{12}$ and PAR4 expression via NF-κB signaling. Moreover, increased activation of SGK1 is accompanied by higher platelet $[Cl^-]_i$ and platelet hyperactivity in CAD, suggesting an important role for Cl^- sensitive, SGK1-dependent pathways in the regulation of platelet function during CAD. The role of SGK1 in thrombus formation has been demonstrated in SGK1 global knockout mice [33]. Here, the mechanistic link between SGK1 and platelet aggregation caused by CFTR-mediated Cl^- transport is further supported by the observation that the specific SGK inhibitor, GSK-650394, effectively counteracted the enhanced platelet activation and aggregation in $Cftr^{PKO}$ mice. These results suggest that elevated $[Cl^-]_i$ may serve as a novel "second messenger" linking extracellular disease-relevant stimuli to the downstream $[Cl^-]_i$-sensitive signaling pathways.

Although SGK1 is implicated in granule biogenesis in platelets from SGK1 global knockout mice, $Cftr^{PKO}$ mice showed no differences in the number of α-granules and dense granules. SGK1 phosphorylation activates NF-κB and regulates downstream platelet signaling pathways. The effects of platelet-specific Cftr knockout on platelet activation through SGK1/NF-κB may bypass granule biogenesis in platelets. Although the results from $Cftr^{PKO}$ and $Cftr^{POE}$ mice provide strong platelet-specific evidence that platelet $[Cl^-]_i$ changes resulting from genetic intervention of CFTR can regulate SGK1 activity, evidence of SGK1 mediating platelet $[Cl^-]_i$ and activation and aggregation is currently unavailable in human research. Taken together, our results suggest a novel Cl^--sensitive, SGK1-dependent mechanism of platelet activation and aggregation associated with thrombosis generation during CAD.

Our in vivo and in vitro results further demonstrate that SGK1 transduces the abnormal $[Cl^-]_i$ signal to the subsequent platelet activation pathway. Activation of NF-κB signaling is an upstream regulator of $P2Y_{12}$ and the PAR4-mediated platelet activation signaling pathway. Recently, we reported that NF-κB signaling pathways increase $P2Y_{12}$ expression in platelets from subjects with diabetes [31]. Meanwhile, our current results reveal that platelet $[Cl^-]_i$ changes, induced by CFTR, modulate the expression levels of $P2Y_{12}$ and PAR4 via SGK1/NF-κB signaling, which is consistent with the findings that SGK1 activates NF-κB in megakaryocytes. SGK1 can upregulate CFTR in airway epithelial cells and, thus, may contribute to epithelial chloride secretion [34]. However, neither $S422^D$ nor $S422^A$ affects CFTR expression or the $[Cl^-]_i$ in MEG-01 cells (Fig. 7c, d). The co-transfection of CFTR overexpressing adenovirus and $S422^D$ restored the platelet activation signaling cascade (Fig. 7e, f), which supports the notion that SGK1 is a downstream kinase of CFTR in platelet activation signaling pathways and suggests that CFTR deficiency promoted platelet activation via the $[Cl^-]_i$-activated SGK1 signaling pathway.

$P2Y_{12}$ and PAR4 play a central role in platelet activation and are the major antiplatelet targets. Herein, the screening of platelet surface proteins revealed the upregulation of $P2Y_{12}$ and PAR4 on

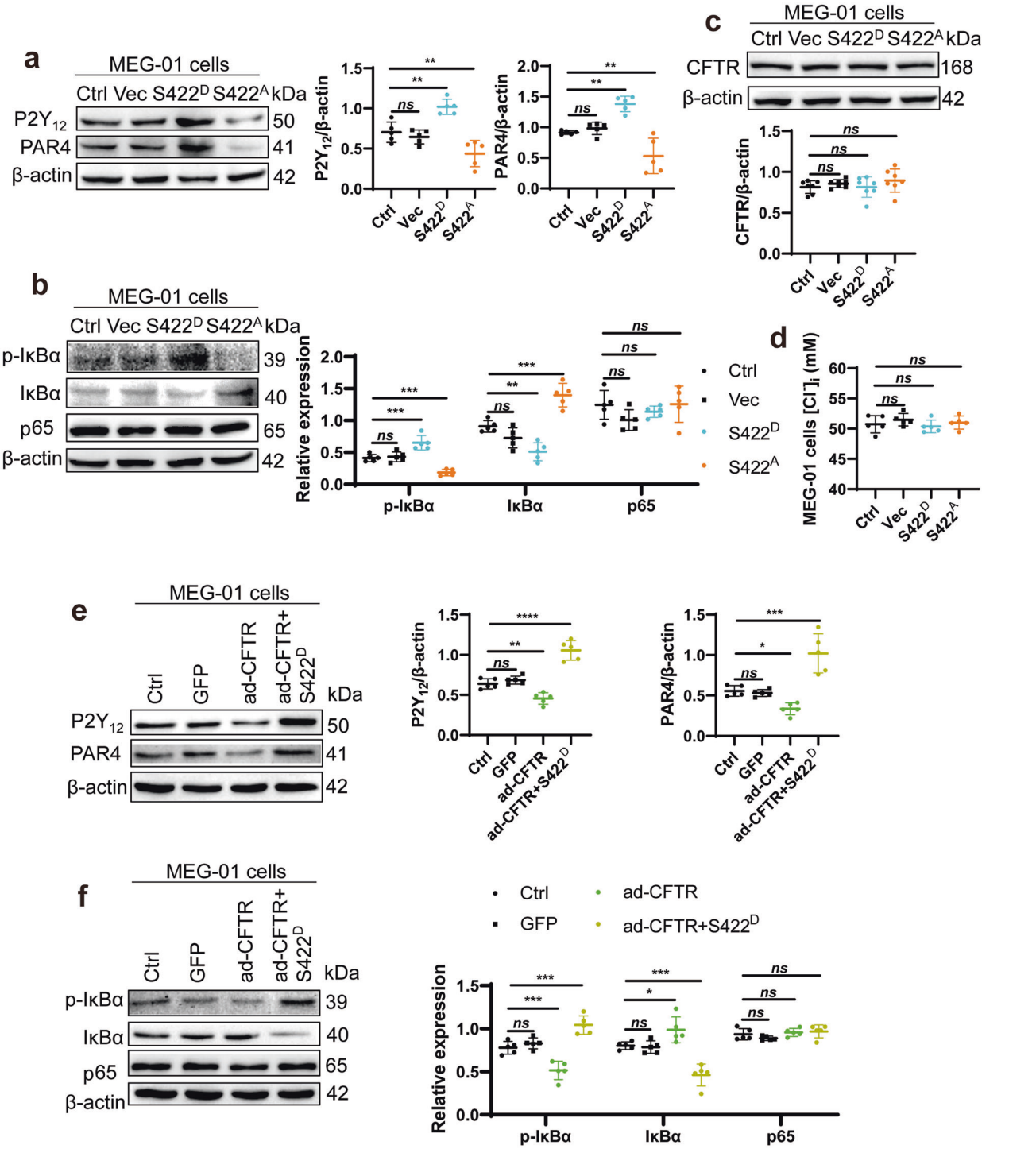

Fig. 7 SGK1 transduces the $[Cl^-]_i$ signal from decreased CFTR to downstream NF-κB/$P2Y_{12}$ and PAR4 activation. a MEG-01 cells were treated with active mutant $S422^D$ of SGK1 or inactive mutant $S422^A$ of SGK1for 48 h, respectively, and the expression of $P2Y_{12}$ and PAR4 was analyzed using Western blotting. ($n = 5$ independent experiments; one-way ANOVA). **b** Immunoblot analysis of effects of $S422^D$ or $S422^A$ on IκBα, p-IκBα, and NF-κB p65 in MEG-01 cells ($n = 5$ independent experiments; one-way ANOVA). **c** Western blot images showing CFTR expression in MEG-01 cells transfected with $S422^D$ or $S422^A$ mutant ($n = 7$ independent experiments; one-way ANOVA). **d** MEG-01 cells $[Cl^-]_i$ transfected with $S422^D$ or $S422^A$ mutant was measured using the MQAE probe ($n = 5$ independent experiments; one-way ANOVA). **e** Immunoblot analysis indicating effects of transfection with ad-CFTR alone or co-transfection with ad-CFTR and $S422^D$ on expressions of $P2Y_{12}$ and PAR4 in MEG-01 cells ($n = 5$ independent experiments; one-way ANOVA). **f** Immunoblot analysis indicating effects of ad-CFTR or ad-CFTR and $S422^D$ on IκBα, p-IκBα, and p65 in MEG-01 cells ($n = 5$ independent experiments; one-way ANOVA). Data are presented as mean ± SEM; $^*P < 0.05$, $^{**}P < 0.01$, $^{***}P < 0.001$, and $^{****}P < 0.0001$. ns not significant

$Cftr^{PKO}$ platelets. Moreover, stimulation of $P2Y_{12}$ receptors by ADP amplifies the activation response to other platelet activators (such as fibrinogen, fibronectin, and vitronectin) resulting in sustained aggregation and secretion; hence, $P2Y_{12}$ receptor inhibitors effectively reduce ischemic risk in CAD management [35]. Thrombotic factors, such as fibrinogen, fibronectin, and vitronectin, should be investigated in CFTR genetically modified mice [36–39]. Our results also show that Cl^--sensitive SGK1 phosphorylation and its downstream $P2Y_{12}$ and PAR4 expression are upregulated in platelets from patients with CAD. Hence, CFTR abundance, as well as its mediated $[Cl^-]_i$ abnormality in platelets, may function as a potential predictor for thrombotic events in patients with CAD. Platelet activation is a common pathogenic mechanism underlying not only thrombosis, but also thrombo-inflammation in cardiovascular events [1, 40, 41]. Thus, restoring normal $[Cl^-]_i$ by increasing CFTR expression is a potential anti-thrombotic approach for the prevention and treatment of cardiovascular events in CAD.

Recently, Ortiz-Munoz et al. confirmed the essential role of CFTR in CD62P expression, showing that CFTR deficiency results in increased platelet activation using similar platelet-specific Cftr-knockout mice [14]. However, Cftr-knockout mice in this study displayed normal platelet aggregation in response to thrombin and collagen. The differences between Ortiz-Munoz's results and our results may be attributed to the different dosage range of thrombin tested. We found that a lower thrombin dosage significantly increased the platelet aggregation rate in $Cftr^{PKO}$ mice while eliciting the opposite effect in $Cftr^{POE}$ mice (Figs. 3b, 4d). However, the higher dosage of thrombin did not affect the platelet aggregation rate in any group. Furthermore, the findings in $Cftr^{PKO}$ mice exposed to $FeCl_3$ suggest a critical role for Cftr- knockout platelets in the worsening of thrombosis. Increased $P2Y_{12}$, PAR4, and P-selectin expression, enhanced ATP secretion, and activated NF-κB signaling contributed to the increased thrombosis risk in CAD, which was also observed in $Cftr^{PKO}$ mice. Conversely, platelet-specific CFTR overexpression ($Cftr^{POE}$) lowered mouse platelet $[Cl^-]_i$ and decreased platelet activation and thrombus generation induced by $FeCl_3$. Therefore, the present study provides strong evidence supporting the critical role of CFTR in thrombosis.

The abnormal $[Cl^-]_i$ in Cftr-knockout and -overexpressing mice is consistent with the findings of previous studies using global Cftr-knockout mice, supporting the notion that Cl^- signaling may contribute to platelet hyperactivation and subsequent platelet-mediated inflammation in CF [13, 14]. Interestingly, several CAD risk factors have been associated with patients with CF, including respiratory tract inflammation, strong oxidative stress, multifaceted lipid abnormalities, endothelial dysfunction, and platelet hyperactivation, which have attracted considerable interest in terms of investigating the prevalence of CAD in patients with CF [42]. However, data regarding CAD and/or its risk factors in patients with CF are limited since patients with CF do not generally survive to middle age before the advent of CFTR correctors/potentiators (e.g., Ivacaftor (VX-770)). Our study demonstrated that platelet $[Cl^-]_i$ is closely associated with increased thrombosis risk in patients with CAD. Moreover, $Cftr^{POE}$ significantly reduced platelet activation and thrombus generation by decreasing $[Cl^-]_i$ -dependent SGK1 signaling. This finding suggests decreased endogenous CFTR protein expression in CAD platelets as a novel target for the development of anti-thrombotic therapies regulating abnormal $[Cl^-]_i$ and subsequent changes. Our results, together with recent findings demonstrating that clinical CFTR correctors/potentiators successfully enhance CFTR-mediated Cl^- transport in non-CF cells, suggest the restoration of CFTR-mediated platelet $[Cl^-]_i$ as a potential anti-thrombotic therapeutic strategy [43]. Therefore, $[Cl^-]_i$ may be a potential biomarker of thrombosis risk, with CFTR as a novel potential therapeutic target for CAD and other arterial thrombosis-related cardiovascular diseases, such as stroke. Notably, the mRNA and protein levels of CFTR in platelets from patients with CAD were significantly lower than those in NCA subjects. Both CFTR genetic intervention and pharmacological inhibition of CFTR chloride channels induce increased thrombus formation in an $FeCl_3$-induced mesenteric arteriole thrombosis model, while enhancing platelet aggregation and ATP secretion. Thus, our findings have expanded on the previously recognized pathological role of the CFTR chloride channel beyond its activity to also include the effect elicited upon its decreased abundance.

This study has some limitations. First, the thrombosis model itself was limited. The $FeCl_3$ injury induces endothelial cell denudation and exposure of subendothelial matrix proteins, which mimics some pathophysiological conditions of arteries in CAD, such as rupture of atherosclerotic plaque and artery trauma [44]. The currently used models of arterial thrombosis have major drawbacks when exploring the pathophysiological role of platelets in CAD. Considering that arterial thrombosis is induced in the absence of atherosclerotic lesions, no model can truly mimic human pathological states during CAD. The results obtained from human research are in line with those from $FeCl_3$-indcued thrombosis model in platelet-specific Cftr knockout mice. Therefore, our study suggests that platelet-specific Cftr knockout mice can mimic, to some degree, clinical platelet hyperactivity during CAD. To determine the degree in which CFTR genetic intervention mimics CAD phenotype, $Cftr^{PKO}/ApoE^{-/-}$ and $Cftr^{POE}/ApoE^{-/-}$ atherosclerotic mouse models should be constructed to investigate the influence of platelet-specific Cftr genetic intervention on the pathogenesis of CAD. Second, differences among participants in the NCA and CAD groups (in terms of cardiovascular medications, total cholesterol, LDL and HDL levels, and blood platelet count; Table S2) made it difficult to examine the association between CFTR and arterial thrombosis formation in CAD in the same clinical-experimental conditions. Nevertheless, we have made every effort to provide the most relevant data supporting that CFTR-mediated $[Cl^-]_i$ regulates arterial thrombus formation. This association remains to be experimentally strengthened, and we recommend that more clinically relevant models should be employed in future studies.

In conclusion, we demonstrated that elevated $[Cl^-]_i$, due to decreased CFTR expression, may have a critical role in activating platelets and inducing formation of arterial thrombosis via a SGK1-dependent pathway in CAD patients. Specifically, we have shown that Cl^--sensitive SGK1 activity, which is required for CFTR-mediated platelet activation, is significantly enhanced in CAD patients and $Cftr^{PKO}$ mice. The increased $[Cl^-]_i$ activates SGK1, which in turn upregulates NF-κB and downstream $P2Y_{12}$ and PAR4 signaling. Conversely, Cftr-overexpressing platelets showed attenuated activation and arterial thrombosis via reduced $[Cl^-]_i$. Our results demonstrate $[Cl^-]_i$ as a potential biomarker of thrombosis risk, with CFTR may represent a novel antiplatelet target for thrombotic diseases.

ACKNOWLEDGEMENTS

This study was supported by the National Natural Science Foundation of China (82073848 and 81773722 to GLW, 82170231 to CZL, 81803522 to LH, 81903687 to LYZ, 62172452 to RMW, 82104160 to NP); The Science and Technology Program of Guangzhou City (No.201803010092 to GLW; China); Guangdong Natural Science Foundation (No. 2020A1515010045 to LYZ; China); Guangdong Provincial Department of Science and Technology (No.2017A020215104 to LYZ; China). The authors thank Dr. Zhong-ren Ding from the First Affiliated Hospital of Zhengzhou University, Cardiovascular Institute of Zhengzhou University for technical assistance. The authors thank Dr. Heyu Ni from St. Michael's Hospital, University of Toronto for valuable suggestions and comments during the manuscript preparation.

AUTHOR CONTRIBUTIONS

GLW, BZ, CZL, and HYY designed the study. HYY, CZ, LH, and CL performed the experiments and analyzed the data. NP, ML, HH, YZ, JL, LYZ, YSL, BZL, XQH, XFL, ZCL,

JL, ZHL, and RMW assisted with the experiments. GLW, HYY, CZL, LH, and LW wrote the manuscript. YYG and BZ provided valuable suggestions. All authors have approved the final article.

ADDITIONAL INFORMATION

Supplementary information The online version contains supplementary material available at https://doi.org/10.1038/s41401-022-00868-9.

Competing interests: The authors declare no competing interests.

REFERENCES

1. Jackson SP. Arterial thrombosis—insidious, unpredictable and deadly. Nat Med. 2011;17:1423–36.
2. Xu XR, Zhang D, Oswald BE, Carrim N, Wang X, Hou Y, et al. Platelets are versatile cells: new discoveries in hemostasis, thrombosis, immune responses, tumor metastasis and beyond. Crit Rev Clin Lab Sci. 2016;53:409–30.
3. Jackson SP, Schoenwaelder SM. Antiplatelet therapy: in search of the 'magic bullet'. Nat Rev Drug Discov. 2003;2:775–89.
4. Xu XR, Carrim N, Neves MAD, McKeown T, Stratton TW, Coelho RMP, et al. Platelets and platelet adhesion molecules: novel mechanisms of thrombosis and anti-thrombotic therapies. Thromb J. 2016;14:37–46.
5. Li BX, Dai X, Xu XR, Adili R, Neves MAD, Lei X, et al. In vitro assessment and phase I randomized clinical trial of anfibatide a snake venom derived anti-thrombotic agent targeting human platelet GPIbα. Sci Rep-Uk. 2021;11:1–17.
6. Wang M, Yang H, Zheng LY, Zhang Z, Tang YB, Wang GL, et al. Downregulation of TMEM16A calcium-activated chloride channel contributes to cerebrovascular remodeling during hypertension by promoting basilar smooth muscle cell proliferation. Circulation. 2012;125:697–707.
7. Guan Y, Wang G, Zhou J. The ClC-3 Cl^- channel in cell volume regulation, proliferation and apoptosis in vascular smooth muscle cells. Trends Pharmacol Sci. 2006;27:290–6.
8. Testani JM, Hanberg JS, Arroyo JP, Brisco MA, ter Maaten JM, Wilson FP, et al. Hypochloraemia is strongly and independently associated with mortality in patients with chronic heart failure. Eur J Heart Fail. 2016;18:660–8.
9. Naal T, Abuhalimeh B, Khirfan G, Dweik RA, Tang WHW, Tonelli AR. Serum chloride levels track with survival in patients with pulmonary arterial hypertension. Chest. 2018;154:541–9.
10. Harper MT, Poole AW. Chloride channels are necessary for full platelet phosphatidylserine exposure and procoagulant activity. Cell Death Dis. 2013;4:e969.
11. Vaitkevicius H, Turner I, Spalding A, Lockette W. Chloride increases adrenergic receptor-mediated platelet and vascular responses. Am J Hypertens. 2002;15:492–8.
12. O'Sullivan BP, Linden MD, Frelinger AL, Barnard MR, Spencer-Manzon M, Morris JE, et al. Platelet activation in cystic fibrosis. Blood. 2005;105:4635–41.
13. Mattoscio D, Evangelista V, De Cristofaro R, Recchiuti A, Pandolfi A, Di Silvestre S, et al. Cystic fibrosis transmembrane conductance regulator (CFTR) expression in human platelets: impact on mediators and mechanisms of the inflammatory response. FASEB J. 2010;24:3970–80.
14. Ortiz-Muñoz G, Yu MA, Lefrançais E, Mallavia B, Valet C, Tian JJ, et al. Cystic fibrosis transmembrane conductance regulator dysfunction in platelets drives lung hyperinflammation. J Clin Invest. 2020;130:2041–53.
15. Levine GN, Bates ER, Bittl JA, Brindis RG, Fihn SD, Fleisher LA, et al. 2016 ACC/AHA Guideline Focused Update on Duration of Dual Antiplatelet Therapy in Patients With Coronary Artery Disease: A Report of the American College of Cardiology/American Heart Association Task Force on Clinical Practice Guidelines: An Update of the 2011 ACCF/AHA/SCAI Guideline for Percutaneous Coronary Intervention, 2011 ACCF/AHA Guideline for Coronary Artery Bypass Graft Surgery, 2012 ACC/AHA/ACP/AATS/PCNA/SCAI/STS Guideline for the Diagnosis and Management of Patients With Stable Ischemic Heart Disease, 2013 ACCF/AHA Guideline for the Management of ST-Elevation Myocardial Infarction, 2014 AHA/ACC Guideline for the Management of Patients With Non-ST-Elevation Acute Coronary Syndromes, and 2014 ACC/AHA Guideline on Perioperative Cardiovascular Evaluation and Management of Patients Undergoing Noncardiac Surgery. Circulation. 2016;134:e123–55.
16. Zhang Y, Chen P, Guan W, Guo H, Qiu Z, Xu J, et al. Increased intracellular Cl^- concentration promotes ongoing inflammation in airway epithelium. Mucosal Immunol. 2018;11:1149–57.
17. Zhang L, Pathak HR, Coulter DA, Freed MA, Vardi N. Shift of intracellular chloride concentration in ganglion and amacrine cells of developing mouse retina. J Neurophysiol. 2006;95:2404–16.
18. Melis N, Tauc M, Cougnon M, Bendahhou S, Giuliano S, Rubera I, et al. Revisiting CFTR inhibition: a comparative study of CFTRinh-172 and GlyH-101 inhibitors. Br J Pharmacol. 2014;171:3716–27.
19. Voss FK, Ullrich F, Munch J, Lazarow K, Lutter D, Mah N, et al. Identification of LRRC8 heteromers as an essential component of the volume-regulated anion channel VRAC. Science. 2014;344:634–8.
20. Qiu Z, Dubin AE, Mathur J, Tu B, Reddy K, Miraglia LJ, et al. SWELL1, a plasma membrane protein, is an essential component of volume-regulated anion channel. Cell. 2014;157:447–58.
21. Schroeder BC, Cheng T, Jan YN, Jan LY. Expression cloning of TMEM16A as a calcium-activated chloride channel subunit. Cell (Camb). 2008;134:1019–29.
22. Li XY, Lv XF, Huang CC, Sun L, Ma MM, Liu C, et al. LRRC8A is essential for volume-regulated anion channel in smooth muscle cells contributing to cerebrovascular remodeling during hypertension. Cell Prolif. 2021:e13146.
23. Baba K, Shibata R, Sibuya M. Partial correlation and conditional correlation as measures of conditional independence. Aust Nz J Stat. 2004;46:657–64.
24. Budnik A, Henneberg M. Worldwide increase of obesity is related to the reduced opportunity for natural selection. PLoS One. 2017;12:e170098.
25. Caci E, Caputo A, Hinzpeter A, Arous N, Fanen P, Sonawane N, et al. Evidence for direct CFTR inhibition by CFTRinh-172 based on Arg347 mutagenesis. Biochem J. 2008;413:135–42.
26. Gurbel PA, Becker RC, Mann KG, Steinhubl SR, Michelson AD. Platelet function monitoring in patients with coronary artery disease. J Am Coll Cardiol. 2007;50:1822–34.
27. Chen B, Huang C, Lv X, Zheng H, Zhang Y, Sun L, et al. SGK1 mediates the hypotonic protective effect against H2O2-induced apoptosis of rat basilar artery smooth muscle cells by inhibiting the FOXO3a/Bim signaling pathway. Acta Pharmacol Sin. 2020;41:1073–84.
28. Ya-juan Z, Hua-qing Z, Bao-yi C, Lu S, Ming-ming MA, Guan-lei W, et al. WNK1 is required for proliferation induced by hypotonic challenge in rat vascular smooth muscle cells. Acta Pharmacol Sin. 2018;39:35–47.
29. Lang F, Gawaz M, Borst O. The serum- & glucocorticoid-inducible kinase in the regulation of platelet function. Acta Physiol. 2015;213:181–90.
30. Borst O, Schmidt E, Münzer P, Schönberger T, Towhid ST, Elvers M, et al. The serum- and glucocorticoid-inducible kinase 1 (SGK1) influences platelet calcium signaling and function by regulation of Orai1 expression in megakaryocytes. Blood. 2012;119:251–61.
31. Hu L, Chang L, Zhang Y, Zhai L, Zhang S, Qi Z, et al. Platelets express activated P2Y12 receptor in patients with diabetes mellitus. Circulation. 2017;136:817–33.
32. Taylor KA, Wilson DGS, Harper MT, Pugh N. Extracellular chloride is required for efficient platelet aggregation. Platelets. 2018;29:79–83.
33. Walker B, Schmid E, Russo A, Schmidt EM, Burk O, Münzer P, et al. Impact of the serum- and glucocorticoid-inducible kinase 1 on platelet dense granule biogenesis and secretion. J Thromb Haemost. 2015;13:1325–34.
34. Bomberger JM, Coutermarsh BA, Barnaby RL, Sato JD, Chapline MC, Stanton BA, et al. Serum and glucocorticoid-inducible kinase1 increases plasma membrane wt-CFTR in human airway epithelial cells by inhibiting its endocytic retrieval. PLoS One. 2014;9:e89599.
35. Cattaneo M. New P2Y12 inhibitors. Circulation. 2010;121:171–9.
36. Wang Y, Reheman A, Spring CM, Kalantari J, Marshall AH, Wolberg AS, et al. Plasma fibronectin supports hemostasis and regulates thrombosis. J Clin Invest. 2014;124:4281–93.
37. Wang Y, Gallant RC, Ni H. Extracellular matrix proteins in the regulation of thrombus formation. Curr Opin Hematol. 2016;23:280–7.
38. Yang H, Reheman A, Chen P, Zhu G, Hynes RO, Freedman J, et al. Fibrinogen and von Willebrand factor-independent platelet aggregation in vitro and in vivo. J Thromb Haemost. 2006;4:2230–7.
39. Reheman A, Gross P, Yang H, Chen P, Allen D, Leytin V, et al. Vitronectin stabilizes thrombi and vessel occlusion but plays a dual role in platelet aggregation. J Thromb Haemost. 2005;3:875–83.
40. Rondina MT, Weyrich AS, Zimmerman GA. Platelets as cellular effectors of inflammation in vascular diseases. Circ Res. 2013;112:1506–19.
41. von Hundelshausen P, Weber C. Platelets as immune cells bridging inflammation and cardiovascular disease. Circ Res. 2007;100:27–40.
42. Reverri EJ, Morrissey BM, Cross CE, Steinberg FM. Inflammation, oxidative stress, and cardiovascular disease risk factors in adults with cystic fibrosis. Free Radic Biol Med. 2014;76:261–77.
43. Yanda MK, Liu Q, Cebotaru L. A potential strategy for reducing cysts in autosomal dominant polycystic kidney disease with a CFTR corrector. J Biol Chem. 2018;293:11513–26.
44. Lei X, MacKeigan DT, Ni H. Control of data variations in intravital microscopy thrombosis models. J Thromb Haemost. 2020;18:2823–5.